J. COMBIN. MATH. COMBIN. COMPUT. 127a (2025) 8075--8092

Journal of Combinatorial Mathematics and Combinatorial Computing
www.combinatorialpress.com/jcmcc

Combinatorial Press

Calculation and Analysis of Carbon Emission of Ultra-low Energy Consumption Residential Buildings in Frigid Regions Based on the Emission Factor Approach

Lixia Wang[1,✉], Xiaoping Song[2], Zewei Su[1]

[1] *School of Architecture and Surveying & Mapping Engineering, Shanxi Datong University, Datong, Shanxi, 037003, China*
[2] *Datong Architectural Design and Research Institute, Datong, Shanxi, 037006, China*

ABSTRACT

Ultra-low energy buildings for building energy efficiency development, compared with traditional buildings have obvious advantages. This paper simulates ultra-low-energy residential buildings in severely cold regions through Software PHES, and calculates the energy-saving results of ultra-low-energy residential buildings. The carbon emission factor method is analyzed, and the carbon emission factor is calculated at different stages in the life cycle of the building. Select ultra-low-energy residential buildings in cold regions for modeling, input meteorological parameters, indoor environmental parameters and internal disturbance settings, building envelope, and combine with heat recovery system to simulate the operation of ultra-low-energy residential buildings in cold regions. Analyze the indoor and outdoor temperature and humidity values of traditional houses and compare them with those of ultra-low-energy-consumption houses to verify the advantages of ultra-low-energy-consumption residential buildings. Calculate the energy-saving efficiency of ultra-low-energy residential buildings. Using the 9# residential building of Ruihu·Yunshanfu in Datong as a practical verification case, this ultra-low energy residential building has a total life-cycle carbon emission of 171.078 tCO_2/a, with a unit area carbon emission of 16.415 $kgCO_2/m^2 \cdot a$. Compared to the energy-saving design standards implemented in 2016, the carbon emission intensity is reduced by 60.02%, fully confirming the carbon reduction benefits of ultra-low energy residential buildings in severe cold regions.

Keywords: PHES simulation, carbon emission factor, Energy Consumption Analysis, ultra-low-energy residence

✉ Corresponding author.
E-mail address: sxdtwlx2024@163.com (L. Wang).
Received 03 March 2024; Revised 10 May 2024; Accepted 30 November 2024; Published Online 15 April 2025.
DOI: 10.61091/jcmcc127a-444

1. Introduction

With the increasingly serious global climate change and energy crisis, governments and all walks of life are paying more and more attention to energy conservation and emission reduction and improving energy utilization efficiency. In the field of residential buildings, ultra-low-energy retrofit design, as an effective energy-saving measure, aims to reduce the energy consumption level of buildings, reduce carbon emissions and realize sustainable development [1-4]. The emission factor method, which determines the concentration and total amount of air pollutants emitted by measuring and calculating the emission factors of the emission sources, plays an important role in calculating and analyzing the carbon emissions of ultra-low-energy residential buildings in cold regions [5-8].

Ultra-low-energy retrofit design is a technical means to reduce the overall energy consumption level of a building by optimizing the building design, improving the operation efficiency of building equipment, and adopting renewable energy sources under the premise of ensuring the comfort of the building [9-12]. It mainly includes the following aspects: one is to improve the building thermal insulation performance, through increasing the thickness of the building wall insulation materials, set the thermal insulation layer and other measures to reduce the heat loss of the building, improve the building thermal insulation performance [13-15]. The second is to optimize the building lighting design: rationally set the location, area and shape of the windows, improve the natural lighting rate of the building, and reduce the demand for artificial lighting [16-18]. The third is to improve the operation efficiency of building equipment: select equipment with high energy efficiency rating, adopt energy-saving technology to improve the operation mode of equipment, and reduce the energy consumption of equipment [19-21]. The fourth is to adopt renewable energy sources: such as solar photovoltaic power generation, ground source heat pumps, etc., to provide clean energy for buildings and reduce the dependence on fossil energy [22-24].

Literature [25] proposed an optimization method combined with meta-modeling to examine the carbon reduction potential of ultra-low energy buildings in severe cold regions and constructed a building performance meta-model using the XGBoost algorithm. It was highlighted that the optimized GWP, GC and OE were reduced compared to the original building. Literature [26] explored the technical system and economic scheme of ultra-low-energy residential buildings, analyzed the effects of shading and ventilation forms on energy consumption by constructing a typical residential model, and elaborated the incremental cost of ultra-low-energy residential buildings, as well as the value of the promotion of ultra-low-energy buildings. Literature [27] used a probabilistic behavioral model to carry out a multi-objective optimization study of ultra-low-energy residences, and determined the optimal solution for energy saving, indoor thermal comfort and economic cost, which provided a reference for the design of ultra-low-energy buildings in the corresponding areas. Literature [28] analyzed the energy consumption operation monitoring data, aiming to provide a good reference method and design strategy for near-zero energy buildings in cold regions, and provided energy-saving technologies and cost-benefit analysis models for energy conservation in cold regions. Literature [29] proposed a hybrid method combining building energy simulation and orthogonal experiment, and discussed the characteristics of building energy consumption and carbon emission. Conclusions such as "the adoption of renewable energy systems in the operational phase of the baseline building is beneficial to reduce energy consumption" were realized. Literature [30] aims to investigate the carbon emission and reduction potential of low-energy buildings in cold regions. It was pointed out that zero or negative carbon emissions can be achieved in wood frame systems. The sensitivity of carbon emissions from low-energy buildings to incremental photovoltaic (PV) power generation is significantly higher than the replacement rate of recycled concrete. Literature [31] pointed out that ultra-low-energy building is an effective measure to reduce building energy consumption and carbon dioxide emissions in high-cold and high-altitude regions of China, and examined the performance of ultra-low-energy building based on case studies to reveal the difference between its two states of unheated and heated. Literature [32] established a simplified model of panelized residential units in cold regions and fitted the relationship between wall and roof heating factors and regional latitude, showing the correctness of this fitting relationship and laying the foundation for fast and accurate estimation of solar heating potential in cold regions. Literature [33] proposes a construction strategy model for the implementation path of ultra-low-energy buildings applicable to different climate zones and building types, and the recommendations based on the model are of practical value in guiding decision makers to promote the development of ultra-low-energy buildings. The above studies not only show that ultra-low energy residential buildings are widely used in cold regions, but also reveal their importance in favor of energy conservation and emission reduction. Unfortunately, no scholars have mentioned the carbon emission calculation and analysis of ultra-low-energy residential buildings based on the emission factor method in their research. It is noteworthy to point out that in 2021, total carbon emissions from building activities in all phases of China's lifecycle totaled 4.07 billion tons of CO_2, accounting for 38.2% of China's total energy-related carbon emissions and a 4.8% increase from 2020 [34]. Due to the huge influence of this sector, controlling emissions in this sector is crucial to meet China's dual carbon targets. On October 21, 2021, the General Office of Communist Party of China Central Committee published the 'Opinions on Promoting Green Development in Urban and Rural Construction,' calling for the adoption of measures for peaking and achieving carbon neutrality in construction and promoting ultra-low-energy, near-zero-energy, and zero-carbon buildings and developing extensive high-quality green buildings [35]. Compared to conventional green buildings, ultra-low-energy buildings can save as much as 90% of energy and thus greatly reduce emissions and promote timely peaking and realization of dual carbons in the construction sector [36].

This paper analyzes the carbon emission factor method and lists the calculation methods of carbon emission factors at different stages through the life cycle of buildings. The model of ultra-low-energy-consumption residence is established, and various types of building indexes are analyzed by PHES and meteorological parameters, indoor environmental parameters of rooms, as well as internal disturbance settings and envelope settings are brought in, and the heat recovery system is considered to simulate the energy consumption of ultra-low-energy-consumption residence buildings in severe cold areas during the period of use. Compare the thermal environments of traditional and ultra-low-energy-consumption residential buildings, and analyze the temperature and humidity in the two environments. Simulate the results of energy consumption of ultra-low-energy residential buildings in cold regions for a whole year.

2. Methodology for calculating carbon emissions from residential buildings

2.1. Carbon Emission Factor Approach

That is, the construction process energy consumption estimation method. It refers to the method of utilizing the average value of carbon emissions generated during the production of unit products as the basis for calculating the total carbon emissions under normal conditions of management capability and technology level.

At this stage, the carbon emission coefficient is mainly counted in two ways: with gas recovery and without gas recovery. In the specific application of the carbon emission factor, it is mainly based on the energy consumed by the construction machinery when it is used in the construction site. Building construction requires different construction processes to utilize different machinery and equipment to complete the construction of an organic coordinated combination. For different construction processes, the degree of machinery utilization is also different. Therefore, in order to calculate the amount of energy consumed per unit of floor area under different construction methods, it is necessary to know the carbon emissions of different machinery used under different construction techniques. Ultimately, the carbon emissions per unit of floor area are calculated to obtain the amount of energy consumed by the construction process under the total floor area. Finally, the use of different energy sources with different carbon emission coefficients, combined with the corresponding formula to calculate the construction process, the unit area of energy consumption. Finally, calculate the carbon emission under the construction process.

The specific ideas are: first of all, more specific construction process for scientific division. Separately obtain different construction process stages, different equipment use list, including the stage of the use of equipment models, power, quantity and operating time and other data.

Secondly, using the data obtained in the previous stage, according to the above calculation method in this paper, the energy consumption of each construction section is derived from the industrialized residential assembly construction method compared with the traditional residential cast-in-place construction method, and the difference is mainly reflected in the number of building materials used, the energy consumption of construction machinery, the energy consumption of dust and noise reduction facilities, and garbage emissions and other differences.

The basic idea of the emission factor method is to follow the carbon emission inventory list. For each emission source, activity data and emission factors are constructed, which are multiplied together to form a formula for calculating carbon emissions, as shown in (1):

$$Emissions = AD \times EF \tag{1}$$

Where Emissions is the GHG emissions, AD is the activity data (the amount of specific uses and inputs of individual sources that are directly related to carbon emissions), and EF is the emission factor (the amount of GHG released per unit of use of a given source). The total carbon emissions for the building construction measurement period is the sum of the products of the activity data of all emission sources.

Emissions Source 1: ADl x EFl = Emissions l.

Emissions source 2: AD2 × EF2 = Emissions 2.

Emission source n: ADn×EFn=Emissions n.

Total carbon emissions are shown in equation (2):

$$E = \sum_{i=1}^{n} ADi \times EFi \tag{2}$$

2.2. Building life cycle carbon emission factors

The concept of "carbon emission factor" described in this paper is derived from the "carbon emission factor" in the carbon emission factor method. The Intergovernmental Panel on Climate Change (IPCC) defines the carbon emission factor as the amount of carbon emissions produced per unit of energy in the combustion or use of a certain energy source, i.e., carbon emissions $T = \Sigma$ consumption of energy source i × carbon emission factor of energy source i (of which i denotes the energy source category) [34-35].

Indeed, direct or indirect CO2 emissions at all stages of a building's life cycle are ultimately generated by the consumption of energy. However, using energy consumption as an indicator to measure the coincidental emissions of the life cycle of a building retroactively will make the calculation very cumbersome, and will also lead to the problems of unclear division of phases, duplication or omission of calculations, and so on.

In summary, this paper summarizes the carbon emission factors into four categories: energy carbon emission factors, building materials carbon emission factors, transportation carbon emission factors and mechanical equipment carbon emission factors.

In order to realize the calculation function of building life cycle carbon emission factor library system and improve the practicability of the system, this paper formulates the calculation method of building life cycle carbon emission according to the principle of process boundary division based on the carbon emission factor method as follows:

$$E = E_1 + E_2 + E_3 + E_4 + E_5 \tag{3}$$

where E is the total building life cycle carbon emissions (unit: t). $E_1, E_2 \cdots\cdots E_s$ is the carbon emissions from building materials use, building materials transportation, building construction, building operation and maintenance, building demolition and building materials recycling (unit: t), respectively.

(1) Carbon emission calculation formula for building materials production:

$$E_1 = \sum_{i=1}^{n} M_i \times F_{BM,i} \tag{4}$$

where M_i represents the amount of building materials used in Category i. $F_{BM,i}$ represents the carbon emission factor for the production of building materials in category i. By default, all types of building materials are commodities or prefabricated products.

(2) Calculation formula for carbon emissions in the transportation phase of building materials:

$$E_2 = \sum_{i=1, p=1}^{n} F_{T,p} \times B_i \times L_i \tag{5}$$

In the formula, $F_{\tau,p}$ indicates the carbon emission factor for the transportation of building materials when using p types of transportation modes (e.g. road transportation by diesel trucks, electric locomotive transportation, etc.). B_i indicates the total weight of building materials of category i (unit: t), and L_i indicates the distance of building materials of category i from the place of origin to the construction site (unit: km).

(3) Carbon emission calculation formula for the construction phase of the building:

$$E_3 = \sum_{j=1}^{n} F_{MC,j} \times X_j \times N_j \tag{6}$$

where $F_{uc,j}$ represents the carbon emission factor of the construction machinery and equipment in category j. X_j represents the total workload (unit: shift) of category j mechanical equipment, and N_j represents the number of category j mechanical equipment.

(4) Calculation formula for carbon emissions in the operation phase of the building:

$$E_4 = (Q_1 \times F_{EE} + Q_2 \times F_{EF,g} + Q_3 \times F_{EF,l}) \times Y + \sum_{t=1}^{n} R_t \times F_{BM,t} \times C_t \tag{7}$$

In the formula, Y indicates the service life of the building (unit: year). Q_i represents the average annual electricity consumption of the building (unit: kwh), and F_{EE} represents the carbon emission factor of electricity. Q_z indicates the average annual natural gas consumption of the building (unit: m^3), and $F_{EF,g}$ indicates the carbon emission factor of natural gas. Q_3 indicates the average annual amount of liquefied petroleum gas used in the building (unit: Kg), F_{EFJ} indicates the carbon emission factor of liquefied petroleum gas. R_r indicates the amount of building materials to be replaced in Category t (unit: varies by material), $F_{BM,t}$ indicates the carbon emission factor of building materials to be replaced in Category t, and C_t indicates the number of times building materials in Category t are replaced.

(5) Calculation formula for the phase of building demolition and recycling of building materials:

$$E_s = \sum_{q=1}^{n} F_{MC,q} \times X_q \times N_q + \sum_{k=1}^{n} F_{T,k} \times T_k \times D_k + \sum_{s=1}^{n} M_s \times w_s \times (F_{RP,s} - F_{BM,s}) \quad (8)$$

where $F_{MC,q}$ represents the carbon emission factor of the dismantling machinery and equipment in category q. X_q represents the total workload of the demolition machinery and equipment in category q (unit: shift), N_q represents the number of machinery and equipment in category q. $F_{\tau,k}$ represents the carbon emission factor for transportation of building materials in category k, T_k represents the total mass of construction waste in category k (unit: t). D_k denotes the distance (in km) that construction waste or recyclable building materials of category k are transported from the site to the waste recycling site or the building materials processing site. M_s indicates the total mass of recyclable building materials of category s (unit: t), and w_s indicates the recycling factor of category s. $F_{RP,s}$ indicates the carbon emission factor for reprocessing of recyclable building materials in category s, and $F_{BM,s}$ indicates the carbon emission factor for production of recyclable building materials in category s.

3. Simulation of energy consumption in ultra-low-energy homes

3.1. Modeling

The Ruihu-Yunshanfu residential project in Datong City serves as a demonstration of passive ultra-low-energy prefabricated housing in Shanxi Province. The development incorporates structural designs and building materials fully compliant with passive house standards. The building features high-performance thermal insulation, airtight envelopes, and dedicated outdoor air systems (DOAS) with energy recovery units for winter heating. Renewable energy integration includes rooftop photovoltaic (PV) systems for on-site electricity generation.

Taking Building 9 as a case study, this south-facing structure incorporates a reinforced concrete bundle shear wall system with 15 above-grade stories (total height 47.8m) and 2 basement levels (depth 6.6m). The above-ground floor height is 3.1 m, while the underground levels are 3.3 m high. The building has a total floor area of 9,830.05 m^2 (above-ground) and 1,312.93 m^2 (underground), with a 50-year design service life. Divided into two units, each unit contains dual-running parallel staircases, a fire elevator, and a passenger elevator serving two households per floor (total 60 units). The building has a form factor of 0.28, with fenestration ratios per orientation detailed in Table 1. Energy consumption simulations for the 15 above-ground stories were conducted using PHES (Passive House Energy Simulation) software developed by Beijing Green Building Software Co., Ltd.

Table 1. The building faces the window wall ratio

Face	Window ratio
South to (including the balcony door section)	0.43
East direction	0.31
Westward	0.03
North direction	0.02

3.2. PHES Energy Consumption Simulation

The Passive House Energy Simulation (PHES) software is built on the AutoCAD platform, enabling conversion of existing architectural documents into parametric models while providing tools for model creation and modification. The system generates multi-view drawings including floor plans, elevations, and sections. Key features include thermal parameter settings for room functions, equipment specifications, building envelope constructions, external window shading devices, and boundary conditions, forming a comprehensive thermal analysis model.

Based on the Chinese Ultra-Low Energy Residential Building Energy Efficiency Standard, the software performs energy simulations by inputting building geometry, hourly temperature setpoints, and operational schedules. It outputs hourly room temperature profiles and detailed energy consumption breakdowns, calculating primary energy consumption, heating/cooling loads, and renewable energy utilization. The simulation results verify compliance with prescriptive standards and evaluate whether the building achieves ultra-low energy performance targets.

3.3. Meteorological parameter input

Datong City, Shanxi Province (40.12°N latitude, 113.30°E longitude) falls within China's Severe Cold Zone C according to the GB 50176 Thermal Design Code for Civil Buildings. Characterized by long, harsh winters and brief hot summers, the city's annual dry bulb temperature distribution is presented in Figure 1. From June to September, daily average temperatures range between 20°C and 30°C (maximum daily average ⩽30°C), while spring/autumn averages 10-15°C. Winter temperatures span -20°C to -5°C, with minimum daily averages not exceeding -20°C.

Monthly solar irradiance profiles are shown in Figure 2. Solar irradiance increases gradually from January, peaking between June and August when global horizontal irradiance (GHI) exceeds 650 MJ/m^2 and direct normal irradiance (DNI) surpasses 500 MJ/m^2. After August, irradiance levels decline progressively, reaching annual minima in January and December with GHI ⩽250 MJ/m^2 and DNI ⩽200 MJ/m^2.

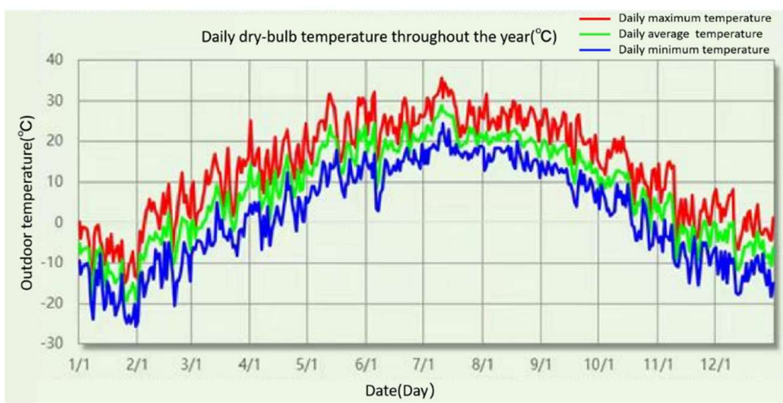

Fig. 1. The city's annual dry bulb temperature statistics

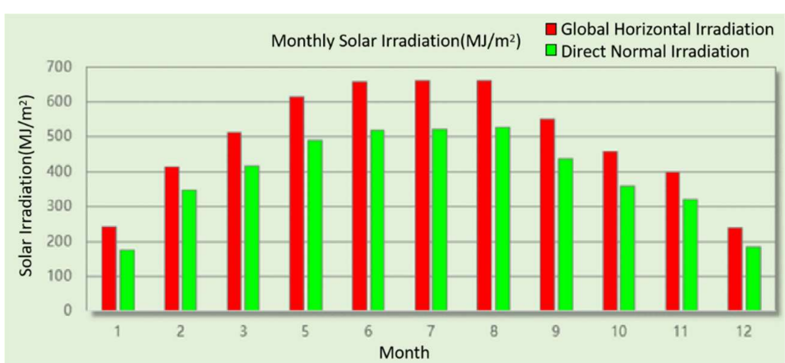

Fig. 2. The city's annual solar irradiance statistics

3.4. Indoor Environmental Parameters and Internal Disturbance Settings

1) Indoor environmental parameter settings. In Datong City, the heating period lasts from October 15th to April 1st of the following year, and the cooling period is from July 10th to August 10th. All windows are kept closed during the heating period. According to the provincial standards regarding indoor parameters, the indoor air - conditioning temperature is set at 20°C in winter and 26°C in summer. There is no heating requirement for stairwells, equipment rooms, and corridors. Based on the actual energy - consumption mode, the daily operation of air - conditioning and heating systems is synchronized with the indoor occupants' activities.

2) Internal disturbance settings. In the energy consumption calculation, the human body, equipment, lighting fixtures, etc. should be operated continuously according to the air conditioning, and at the same time need to take into account the rate of personnel in the room, the lighting utilization rate, the density of equipment use and other factors. Different room personnel, equipment, lighting endothermic settings are shown in Table 2.

Table 2. Different room personnel, equipment, lighting internal heat setting

Type	The per capita area of the land is occupied m^2	Equipment power density W/m^2	Lighting power density W/m^2
Living room	35	6	6
Bedroom	35	7	5
Dining room	35	6	5
Kitchen	35	25	6
Washroom	35	0	5
Uncontrolled temperature	0	0	0

3.5. Settings for Building Envelope and Supporting Facilities

3.5.1. Parameter Settings for the Performance of the External Envelope. Building 9 of Yunshanfu is a demonstration project of passive ultra-low-energy prefabricated residential buildings in Datong City. The project adopts structural designs and building materials that fully meet the requirements of passive ultra-low-energy buildings. An external wall insulation system is employed. For wall details such as parapets, eaves, cantilevered slabs, moldings, plinths, window wells, and air intake and exhaust ducts, thermal break insulation measures are taken. The external doors and windows are made of aluminum-wood composite materials with insulating glass. The heat transfer coefficients of the building envelope and the insulation practices are shown in Table 3. The air-tightness grade of the external windows and doors is Grade 8. The model building is not equipped with shading facilities.

There is no need to input the performance parameters of the external envelope separately. In the simulation calculation, relevant performance parameters such as the heat transfer coefficients of the external walls and windows can be identified by directly selecting the construction material practice tables for the external walls and windows. PHES will automatically obtain the solar radiation values based on the local climate data.

Table 3. Insulation practices and u-values of fenestration and building envelope

Categories	Insulation specification	U-value (W/(m^2·K))
Roof	300mm-thick graphite expanded polystyrene (EPS)	0.12
Stone-clad exterior walls	300mm-thick rock wool board	0.17
Paint-finished exterior walls	250mm-thick molded graphite EPS	0.15

Ultra-low-energy zone windows/doors	6mm Low-E + 12mm Ar + 6mm Low-E + 12mm Ar + 6mm Low-E	1.0
Exterior wall fire barriers	250mm hydrophobic rock wool board	0.17
Partitions between heated/unheated spaces	25mm SF hydrophobic expanded perlite mortar	1.37
Residential entrance doors	Steel airtight doors	1.1
Unit entrance doors	Aluminum-wood composite glazed exterior doors	1.0

3.5.2. Installed Energy-Consuming Systems. The model building incorporates air conditioning, lighting/elevator systems, domestic hot water, heat recovery systems, and an external photovoltaic (PV) power generation system. Energy consumption calculations for these systems are detailed in Equations (9) – (20) [37].

1) Air Conditioning System. Building 9 of Yunshanfu employs a residential ultra-low temperature heat pump multi-split system for year-round heating and cooling. Based on parameters such as HVAC system type, cooling/heating source type, operation schedule, room type, and system efficiency, the PHES software can simulate and calculate air conditioning energy consumption. The energy consumption calculation formula for air conditioning units is:

$$E_{jz}=\left(\frac{Q_A}{COP_A}+\frac{Q_B}{COP_B}+\frac{Q_C}{COP_C}+\frac{Q_D}{COP_D}\right) \tag{9}$$

$$E_{jz}=\frac{Q}{APF} \tag{10}$$

$$E_{jz}=\frac{Q_C}{SEER} \tag{11}$$

where E_{jz} represents the annual energy consumption of air conditioning (unit: kWh/a). $Q_{A\sim D}$ denotes the cumulative cooling/heating load within the i-th load ratio interval (0–25%, 25–50%, 50–75%, 75–100%) (unit: kWh/a). $COP_{A\sim D}$ is the coefficient of performance corresponding to the i-th load ratio interval. Q is the annual cumulative cooling/heating load (unit: kWh/a). APF represents the annual performance factor. SEER is the seasonal energy efficiency ratio.

The energy consumption of water pumps shall be calculated using the following formula:

$$E_{sb}=q_{\max}\times EC(H)R\times\frac{n_1T_A+n_2T_B+n_3T_C+n_4T_D}{n_0} \tag{12}$$

In the formula, E_{sb} represents the annual energy consumption of the water - pumps (unit: kWh/a). $q_{\max}$ is the peak cooling/heating load of the building borne by the water - pumps (unit: kW). EC(H)R is the electricity - to - cooling/heating ratio of the water - pumps. n_0 is the total number of water - pumps. $n_{1\sim 4}$ is the number of operating water - pumps in each of the four load - rate intervals (0 - 25%, 25 - 50%, 50 - 75%, 75 - 100%). $T_{A\sim D}$ is the operating time (h) of the water - pumps in each of the four load - rate intervals (0 - 25%, 25 - 50%, 50 - 75%, 75 - 100%) (unit: h).

The energy consumption of the air - supply system shall be calculated according to the following formula:

$$E_{sf}=\sum_i W_{sf}\times t_{sf}\times F_{sf}\times 10^{-3} \tag{13}$$

$$W_{sf}=W_s\times V_s \tag{14}$$

In the formula, E_{sf} represents the annual energy consumption of the air supply system (unit: kWh/a). W_{sf} is the power consumption of the air supply system (unit: W). t_{sf} denotes the annual operating hours of ERV units, air handling units, or fan-coil units (unit: h). F_{sf} is the simultaneous usage factor for ERV units, air handling units, or fan-coil units. W_s represents the specific power consumption per unit air volume (unit: W/(m^3/h)). V_s is the fresh air volume, air supply volume of air handling units, or air supply volume of fan-coil units (m^3/h).

2) Domestic Hot Water System. In the model building, each household is equipped with a gas water heater with an efficiency of 89%. The total number of residents in Building 9 is estimated to be 200, and the water consumption quota is 30 L per person per day. Based on the actual operating parameters input for the building's domestic hot water system, such as the number of water - using people, the daily water consumption quota per person, the cold - water temperature, the hot - water temperature, the number of operating days per year, the annual average efficiency of the heat source for the domestic hot water system, and the distribution efficiency of the domestic hot water, the annual heat consumption of the building's domestic hot water is calculated using the following formula:

$$Q_{rp} = \frac{4.187 m q_r C_r (t_r - t_1) \rho_r}{1000} \tag{15}$$

$$Q_r = T Q_{rp} \tag{16}$$

where Q_r represents the annual heat consumption for domestic hot water (unit: MJ/a). Q_{rp} is the hourly average heat consumption for domestic hot water (unit: MJ/h). T denotes the annual operating hours of domestic hot water systems (unit: h). ρ_r is the density of hot water (unit: kg/m^3). m is the number of water - using units (either persons or beds, selected as applicable). q_r represents the hot water consumption quota (unit: L/p·d), as per the current national standard Water - Saving Design Standard for Civil Buildings. t_r is the designed hot water temperature (unit: °C). t_1 is the designed cold water temperature (unit: °C).

The annual energy consumption calculation formula for domestic hot water systems is:

$$E_w = \frac{\frac{Q_r}{\eta_r} - Q_s}{\eta_w} \tag{17}$$

where E_w represents the annual energy consumption of the domestic hot water system (unit: kWh/a). Q_r is the annual heat consumption of domestic hot water (unit: MJ/a). Q_s denotes the heat of domestic hot water provided by the solar system (unit: MJ/a). η_r is the distribution efficiency of domestic hot water, which includes the distribution energy consumption of the hot - water system, pipeline heat loss, heat loss from the secondary circulation and storage of domestic hot water (unit: %). η_w is the annual average efficiency of the heat source for the domestic hot water system (unit: %).

3) Lighting System. For the energy - consumption calculation of the lighting system, corresponding parameters are set according to the room names and calculated using the following formula:

$$E_l = \frac{\sum_{j\sim 1}^{365} \left(\sum_i P_{i\cdot j} A_i t_{i\cdot j} + 24 P_p A \right)}{1000} \tag{18}$$

In the formula, E_l represents the annual energy consumption of the lighting system (unit: kWh/a). $P_{i\cdot j}$ is the lighting power density of the i-th room at time j (unit: W/ m^2). A_i denotes the lighting area of the i-th room (unit: m^2). $t_{i\cdot j}$ is the lighting duration of the i-th room at time j (unit: h). P_p represents the emergency lighting power density (unit: W/m^2). A is the total building area (unit: m^2).

4) Elevator System. The building is equipped with 4 elevators across 2 units, each with a rated load capacity of 1000 kg. The elevator system energy consumption is calculated directly by the software based on input parameters such as the number of elevators, specific energy consumption, annual average operation time, and speed. The calculation formula is:

$$E_e = \frac{3.6 P t_a V W + E_{standby} t_s}{1000} \tag{19}$$

In the formula, E_e represents the annual elevator energy consumption (unit: kWh/a). P is the specific energy consumption (unit: kWh/km·kg). t_a denotes the annual average operating hours (unit: h). V is the elevator speed (unit: m/s). W represents the rated load capacity (unit: kg).

$E_{s\tan dby}$ is the standby energy consumption (unit: W). t_s denotes the annual average standby hours (unit: h).

3.6. High-efficiency heat recovery systems

Heat recovery devices are of great significance for ultra-low energy consumption houses. In the winter of cold and frigid regions, ultra-low energy consumption houses, due to their good airtightness and heat insulation performance, reduce to a certain extent the refrigeration and heating loads caused by the enclosure structure and cold air infiltration, and at this time, the fresh air loads are particularly prominent. This is because of the long winter time and low temperature in cold and cold areas, the temperature difference between indoor and outdoor is large, which also means that the enthalpy difference is large, so the fresh air load accounts for a larger proportion. If a heat recovery system is introduced to recover heat from the exhaust air, the fresh air load can be reduced.

Heat recovery system in the recovery of energy at the same time, increasing the fan operating resistance, which also increases the fan energy consumption, only in the heat recovery of energy (taking into account the unit refrigeration thermal performance coefficient) can offset the heat recovery system itself and increase the energy consumption, the heat recovery system is energy-saving. For example, in summer cooling conditions, when the outdoor air enthalpy is higher than the indoor air enthalpy, and the enthalpy difference is higher than the minimum economic enthalpy difference, open the heat recovery system is energy-saving, otherwise the heat recovery system should be turned off, so that the new air is filtered through the by-pass piping directly into the room. In winter heating conditions, the heat recovery system start and stop is the opposite. The rest of the transition season, the temperature difference between indoor and outdoor is small, the new air is filtered and sent directly to the room through the bypass pipe, without turning on the heat recovery system. The function of each indoor air-conditioning room is the same, which makes the processing state point of each indoor air has similarity, and so does the heat recovery state. When calculating the amount of heat recovery, the state point of indoor air is calculated by the hour-by-hour air enthalpy value of an air-conditioning room, and the enthalpy value of outdoor air is calculated according to the hour-by-hour meteorological parameter.

Taking the unit in the sample room as an example, the unit has a built-in total heat recovery rate of 77.3%, and this value is used as the heat recovery efficiency for both cooling and heating conditions. In addition, when the temperature is low in winter, in order to prevent the condition of freezing and cracking of the metal pipe inside the unit, the unit will add the function of fresh air preheating, and the fresh air inlet in winter is calculated according to preheating to 5℃.

3.7. Photovoltaic (PV) System

Building 9 of Yunshanfu is equipped with a photovoltaic system featuring 580W monocrystalline silicon modules installed on the roof. The system is divided into two inverters for distributed PV power generation, with a net panel area of 277.03 m^2, total capacity of 60 kW, PV cell conversion efficiency of 22.3%, and loss efficiency of 20%.

The annual power generation of the PV system is calculated using the formula:

$$E_{pv} = IK_E(1 - Ks)A_p \tag{20}$$

where E_{pv} represents annual power generation of the PV system (unit: kWh). I is annual solar irradiance on the PV cell surface (unit: kWh/m^2). K_E is PV cell conversion efficiency (unit: %). K_S PV cell loss efficiency (unit: %). A_p Net PV panel area (unit: m^2).

4. Results of energy simulation for ultra-low-energy homes

4.1. Measured analysis of ultra-low-energy homes

4.1.1. Analysis of measured data on energy consumption of conventional dwellings. The test was conducted daily at 16:00 from January 1 to January 31, 2024, with recorded meteorological parameters including a maximum outdoor temperature of 3℃ on January 12, a minimum temperature of −25℃ on January 22, an average temperature of −10.4 ℃ over 31 days, and relative humidity ranging from 50.6% to 85% with an average of 61.4%. The weather conditions during the period were characterized by predominantly sunny/cloudy skies and northwesterly winds (Force 1–3), aligning with the typical cold winter climate in severe cold regions, thus ensuring high objectivity and authenticity of the test results. Figure 3 illustrates the outdoor temperature and humidity variations.

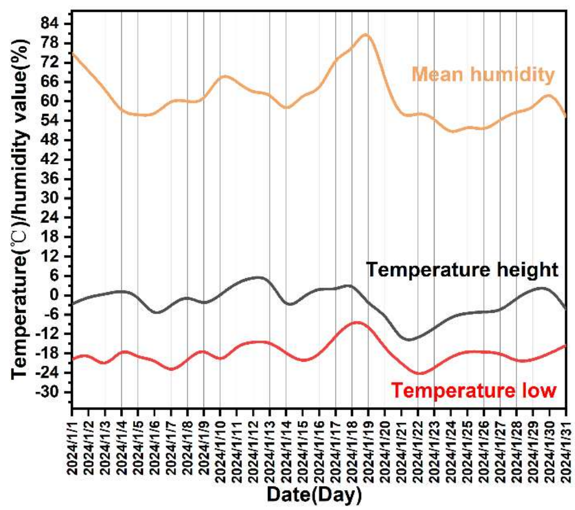

Fig. 3. Change of ambient temperature and humidity in outdoor environment

The indoor thermal environment of the reference house was tested, with temperature and humidity variations presented in Figure 4. Due to the large window openings and lack of insulation in the building envelope, the minimum indoor temperature in the south-facing bedroom of the reference house was only 13.5℃, with an average of approximately 16℃. The living room space recorded a minimum temperature of 12.2℃ due to high accessibility on weekdays, compounded by stronger cold air infiltration resulting from frequent door/window openings and uninsulated building components. At certain times, living room temperatures dropped below 12℃, creating thermal discomfort that negatively affected adjacent bedrooms and necessitated increased fuel consumption for space heating. During extreme cold periods (e.g., January 22), residents were required to operate heating equipment continuously to maintain acceptable indoor temperatures.

Humidity levels in the south-facing bedroom ranged from 22% to 35% (average 30%), with similar conditions observed in the living room.

(a) Temperature variation (b) Humidity variation

Fig. 4. Refer to the change of temperature and humidity in residential indoor

4.1.2. Changes in indoor temperature and humidity in ultra-low-energy homes. The indoor thermal environment of the ultra-low-energy home was tested, and the indoor temperature and humidity variations in the ultra-low-energy home are shown in Figure **5.** n this residence, the building's envelope walls are insulated. And transparent structures such as windows and doors are also made of building components with lower coefficients, and the overall airtightness of the building has been substantially strengthened. The results of the indoor thermal environment measurements show that the average indoor temperature of the bedroom space and living room space on the south-facing first floor of the residence is 24.3°C in winter, and the minimum daily average temperature is 20.7°C. The indoor temperature of the living room space connecting to the entrance hall of the residence is 20.7°C.

The living room space is connected to the entrance gate of the house, under the condition of high thermal insulation of the outer enclosure structure and windows and doors, the living room space does not have strong temperature changes in daily use, and the overall space is weakly infiltrated by the cold wind from the outdoors.

From the test data, the living room space in the use of the process, the lowest point of the indoor temperature of 18.9 ℃. The living room space with a stable thermal environment makes the indoor temperature of the bedroom space and other spaces secure. And under the outdoor conditions where extremely cold temperatures occur in winter, the overall average indoor temperatures of the building are above 23 ℃ and comply with the province's indoor thermal environment indicators. The measured data from Building 9# of Ruihu·Yunshanfu in Datong further confirms the superiority of ultra-low energy homes in severely cold regions. Similar to the test results presented here, this building maintains an average indoor temperature above**23**℃ under severe winter conditions, providing comfort levels far surpassing traditional residences while significantly reducing energy consumption.

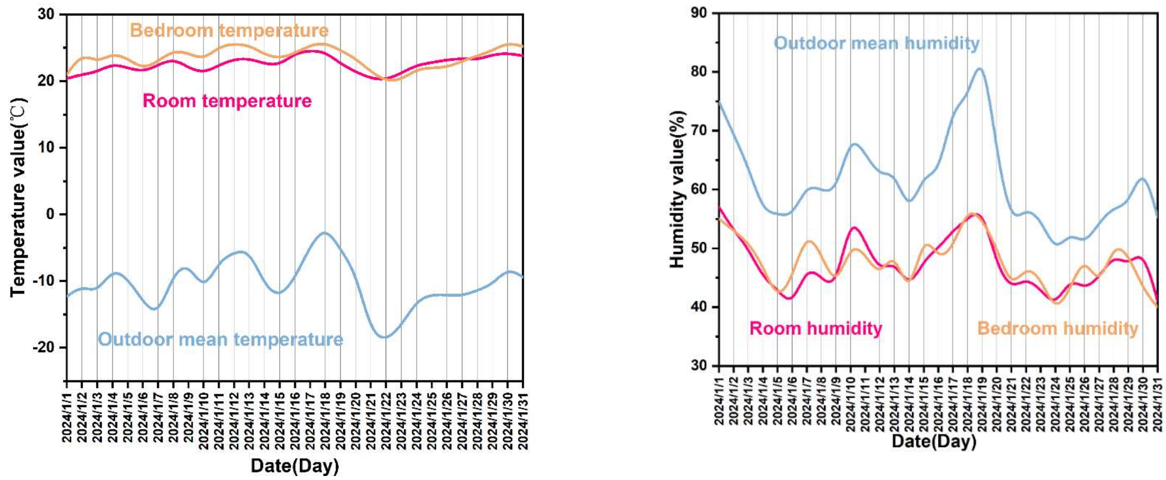

(a) Temperature variation (b) Humidity variation

Fig. 5. The temperature and humidity changes in the indoor indoor temperature

4.2. Energy consumption simulation results

The Green Building Sver PHES (Passive House Energy Simulation software for Very Low Energy buildings) is based on the energy-saving standards for ultra-low energy residential buildings. By inputting basic building data, set temperature values for various time periods, and daily operational schedules, it conducts energy consumption simulations for the building and calculates various energy consumption indicators, including annual heating and cooling loads, primary energy consumption, cooling and heating energy consumption, and renewable energy utilization. Monthly loads throughout the year and a breakdown of the annual load statistics are presented in Tables 4 and 5, respectively.

Table 4. Monthly Loads Throughout the Year

Month	Heating (kWh)	Cooling (kWh)	Peak Heating Load (kW)	Peak Heating Load Time	Peak Cooling Load (kW)	Peak Cooling Load Time
January	46,599	0	127.553	08:00, January 31st	0.000	-
February	15,443	0	92.611	06:00, February 1st	0.000	-
March	7,143	0	59.226	06:00, March 5th	0.000	-
April	3	0	2.591	-	0.000	-
May	0	0	0.000	-	0.000	-
June	0	0	0.000	-	0.000	-
July	0	5,216	0.000	-	210.498	12:00, July 13th
August	0	1,172	0.000	-	71.235	17:00, August 2nd
September	0	0	0.000	-	0.000	-
October	3,542	0	51.770	08:00, October 27th	0.000	-
November	24,098	0	78.307	08:00, November 21st	0.000	-
December	31,256	0	89.911	08:00, December 29th	0.000	-

Table 5. Breakdown and Statistics of Annual Loads

Category	Envelope Heat Transfer	Indoor Heat Gain (kWh/㎡)	Solar Radiation Heat Gain	Heat Loss from Fresh Air Infiltration	Heat Recovery (kWh/㎡)	Total (kWh/㎡)	Heat Recovery Proportion

	(kWh/㎡)		(kWh/㎡)	(kWh/㎡)			
Heating Period	-8.85	14.13	21.03	-117.11	74.29	-16.52	81.9%
Cooling Period	0.22	0.77	0.81	-0.60	-0.30	2.10	12.5%

As shown in Table 5, the heating load in January throughout the year is the highest, reaching 46,599 kWh, while the minimum value in April is 3 kWh. The cooling load peaks in July at 5,216 kWh and is relatively lower in August at 1,172 kWh. According to the simulation results in Table 6, the annual building heating load of 16.52 kWh/㎡ is far greater than the cooling load of 2.10 kWh/㎡. These values are far lower than the requirements specified in the codes, indicating its relatively remarkable energy-saving effect. Among the annual heating loads, the energy consumption for fresh air treatment is the largest, reaching 117.11 kWh/㎡, indicating a relatively high proportion of fresh air energy consumption in the total building energy consumption. The heat recovery from exhaust air is 74.29 kWh/㎡, accounting for a relatively large proportion of 81.8% in the annual heating load. Therefore, reducing fresh air energy consumption and promoting exhaust air heat recovery are effective measures to lower heating energy consumption.

The measured data from Building 9# of Ruihu·Yunshanfu further validates the reliability of the above simulation results. The building's operational heating energy consumption is 87,541.791 kWh/a, representing a 51.41% reduction compared to the reference building; the air-conditioning energy consumption is 22,111.258 kWh/a, a 10.95% reduction compared to the reference building. These significant energy consumption reductions are primarily attributed to the building's efficient exterior wall insulation system and full heat recovery equipment. It is worth noting that the building's lighting energy consumption is 51,703.409 kWh/a, slightly higher than the reference building but accounting for a relatively small proportion of the total carbon emissions.

Particularly noteworthy is that the solar photovoltaic system of Building 9# generates 77,562.67 kWh/a of electricity, resulting in a carbon reduction of 68.589 tCO_2/a, equivalent to 68% of the total carbon emissions during the operation stage, demonstrating the significant effect of renewable energy in building carbon reduction. Table 6 summarizes the carbon emissions at each stage of the building's full lifecycle.

Table 6. Summary of Annual Carbon Emissions by Stage for Building 9# of Yunshanfu

Name	Carbon Emissions (tCO_2/a)	Carbon Emissions per Unit Area ($kgCO_2/m^2{\cdot}a$)	Annual Carbon Emission Ratio (%)
Material Production Stage	76.023	7.293	44.3
Material Transportation Stage	9.754	0.936	5.6
Construction Stage	6.939	0.666	4.0
Greening Carbon Sink	-2.51	-0.241	-1.5
Building Operation Stage	105.741	10.326	62.8
Building Demolition Stage	0.582	0.056	0.3
Recyclable Materials	-25.451	-2.442	-15.0
Total	171.078	16.415	100

5. Conclusion

This paper calculates the energy consumption of ultra-low-energy residential buildings in severe cold regions through carbon factor emissions. The load analysis of ultra-low-energy residential buildings is carried out using Software PHES energy simulation. Meteorological parameters, indoor and outdoor temperatures and humidity of the ultra-low-energy house are measured, and the energy consumption results are analyzed by bringing in the meteorological parameters, indoor and outdoor parameters of the room, and the envelope parameters.

Unlike traditional residential energy consumption, the thermal environment of the ultra-low-energy house keeps the indoor temperature of the bedroom space and other spaces stable, and the overall average indoor temperature of the building is above 23℃ and complies with the indoor thermal environment index.

Utilizing Building 9# in Datong's Ruihu·Yunshanfu as a sample, our result shows that the total life-cycle annual carbon emissions for this building are 171.078 tCO_2 with a per-unit area emission rate of 16.415 $kgCO_2/m^2 \cdot a$. Compared to 2016 energy-saving design specifications, 60.02% reduction in carbon emissions has been achieved, which is well above the 40% required under relevant regulations. This result highlights the large benefits in reducing carbon from ultra-low energy buildings in areas with extremely cold climates.

Empirical research has proven that emissions in the building's operational stage account for the largest share, estimated to be 62.8%. Of all the emissions in this operational stage, heating-related emissions weighing 77.413 tCO_2/a account for 76.7% of all operational emissions, thus being the largest source of such emissions. Additionally, lighting-related carbon emissions are significant in the operational stage and account for 45.5% in total. Carbon emission mitigation through solar power generation is highly effective and has a significant impact, with resultant mitigation being equivalent to 68% of all operational carbon emissions. This highlights the significance of promoting the use of photovoltaic power generation systems in buildings in extremely cold climates as a highly effective method for reducing building-related emissions.

Funding

This work was supported by the Horizontal Project: Simulation and Calculation of Carbon Emissions and Energy Consumption for Building 9# of Yunshanfu Ultra-low Energy Building in Datong City.

References

[1] Hu, Y., Ren, S., Wang, Y., & Chen, X. (2020). Can carbon emission trading scheme achieve energy conservation and emission reduction? Evidence from the industrial sector in China. Energy Economics, 85, 104590.

[2] Zhou, D. Q., Wang, Q., Su, B., Zhou, P., & Yao, L. X. (2016). Industrial energy conservation and emission reduction performance in China: A city-level nonparametric analysis. Applied Energy, 166, 201-209.

[3] Zhong, S., Yingxia, Y., Na, L., & Zhonghua, X. (2017). Energy Consumption Building Design in Tianjin, China. Journal of Clean Energy Technologies, 5(5).

[4] Yang, X., Zhang, S., & Xu, W. (2019). Impact of zero energy buildings on medium-to-long term building energy consumption in China. Energy Policy, 129, 574-586.

[5] Shen, H., Luo, Z., Xiong, R., Liu, X., Zhang, L., Li, Y., ... & Tao, S. (2021). A critical review of pollutant emission factors from fuel combustion in home stoves. Environment international, 157, 106841.

[6] Wang, L., Dai, S., & Wang, C. (2024). Carbon Footprint Accounting and Verification of Seven Major Urban Agglomerations in China Based on Dynamic Emission Factor Model. Sustainability (2071-1050), 16(22).

[7] Levy, P. E., Cowan, N., Van Oijen, M., Famulari, D., Drewer, J., & Skiba, U. (2017). Estimation of cumulative fluxes of nitrous oxide: uncertainty in temporal upscaling and emission factors. European Journal of Soil Science, 68(4), 400-411.

[8] Wang, J. M., Jeong, C. H., Hilker, N., Healy, R. M., Sofowote, U., Debosz, J., ... & Evans, G. J. (2021). Quantifying metal emissions from vehicular traffic using real world emission factors. Environmental Pollution, 268, 115805.

[9] Tong, X., Yang, X., & Ma, X. (2019). Discussion on the Intelligent Design of Ultra-Low Energy Consumption Passive Buildings. Frontiers Research of Architecture and Engineering, 2(2), 20-24.

[10] Amann, J. T. (2014, December). Energy Codes for Ultra-Low-Energy Buildings: A Critical Pathway to Zero Net Energy Buildings. American Council for an Energy-Efficient Economy.

[11] Ma, Y., Deng, W., Xie, J., Heath, T., Ezeh, C. I., Hong, Y., & Zhang, H. (2023). A macro-scale optimisation of zero-energy design schemes for residential buildings based on building archetypes. Solar Energy, 257, 196-209.

[12] Xu, X., Feng, G., Chi, D., Liu, M., & Dou, B. (2018). Optimization of performance parameter design and energy use prediction for nearly zero energy buildings. Energies, 11(12), 3252.

[13] La Rosa, A. D., Recca, A., Gagliano, A., Summerscales, J., Latteri, A., Cozzo, G., & Cicala, G. (2014). Environmental impacts and thermal insulation performance of innovative composite solutions for building applications. Construction and Building Materials, 55, 406-414.

[14] Abu-Jdayil, B., Mourad, A. H., Hittini, W., Hassan, M., & Hameedi, S. (2019). Traditional, state-of-the-art and renewable thermal building insulation materials: An overview. Construction and Building Materials, 214, 709-735.

[15] O'Hegarty, R., Amedeo, G., & Kinnane, O. (2024). The impact of compromised insulation on building energy performance. Energy and Buildings, 316, 114337.

[16] Mansfield, K. P. (2018). Architectural lighting design: A research review over 50 years. Lighting Research & Technology, 50(1), 80-97.

[17] Livingston, J. (2021). Designing with light: The art, science, and practice of architectural lighting design. John Wiley & Sons.

[18] Skarżyński, K., & Żagan, W. (2022). Quantitative Assessment of Architectural Lighting Designs. Sustainability, 14(7), 3934.

[19] Ahn, C. R., & Lee, S. (2013). Importance of operational efficiency to achieve energy efficiency and exhaust emission reduction of construction operations. Journal of Construction Engineering and Management, 139(4), 404-413.

[20] Szamocki, N., Kim, M. K., Ahn, C. R., & Brilakis, I. (2019). Reducing greenhouse gas emission of construction equipment at construction sites: Field study approach. Journal of Construction Engineering and Management, 145(9), 05019012.

[21] Lu, G., Yin, Z., Din, X., & Zhang, J. (2018, July). Research on Key Technology of Ultra-low Energy Consumption Buildings in Beijing. In IOP Conference Series: Materials Science and Engineering (Vol. 381, No. 1, p. 012097). IOP Publishing.

[22] Chel, A., & Kaushik, G. (2018). Renewable energy technologies for sustainable development of energy efficient building. Alexandria engineering journal, 57(2), 655-669.

[23] Sharafi, M., ElMekkawy, T. Y., & Bibeau, E. L. (2015). Optimal design of hybrid renewable energy systems in buildings with low to high renewable energy ratio. Renewable Energy, 83, 1026-1042.

[24] Vares, S., Häkkinen, T., Ketomäki, J., Shemeikka, J., & Jung, N. (2019). Impact of renewable energy technologies on the embodied and operational GHG emissions of a nearly zero energy building. Journal of Building Engineering, 22, 439-450.

[25] Zhang, Z., Wang, W., Song, J., Wang, Z., & Wang, W. (2022). Multi-objective optimization of ultra-low energy consumption buildings in severely cold regions considering life cycle performance. Sustainability, 14(24), 16440.

[26] Bian, J., Ren, N., Xia, W., Zuo, C., Li, Z., Yi, D., & He, M. (2024, November). Impact Analysis of Low Carbon Technologies for Residential Buildings in Hot Summer and Cold Winter Regions. In 2024 6th International Conference on Electrical, Control and Instrumentation Engineering (ICECIE) (pp. 1-5). IEEE.

[27] Xiang, J., Liu, H., Li, X., Jones, P., & Perisoglou, E. (2023). Multi-objective optimization of ultra-low energy housing in hot summer cold winter climate zone of China based on a probabilistic behavioral model. Buildings, 13(5), 1172.

[28] Li, S., Shi, T., Han, B., Li, T., Hao, T., & Dong, Y. (2018, August). Low-carbon building design and practice in severe cold areas. In IOP Conference Series: Materials Science and Engineering (Vol. 399, No. 1, p. 012032). IOP Publishing.

[29] Ke, Z., Liu, X., Zhang, H., Jia, X., Zeng, W., Yan, J., ... & Hien, W. N. (2023). Energy Consumption and Carbon Emissions of Nearly Zero-Energy Buildings in Hot Summer and Cold Winter Zones of China. Sustainability, 15(14), 11453.

[30] Wang, Y., Yang, X., Hou, Q., Tao, J., & Dong, J. (2022). Quantitative study on the life-cycle carbon emissions of a nearly zero energy building in the severe cold zones of China. Sustainability, 14(3), 1448.

[31] Qiang, G., Fuxi, W., Yi, G., Yuanjun, L., Yang, L., & Zhang, T. (2023). Study on the performance of an ultra-low energy building in the Qinghai-Tibet Plateau of China. Journal of Building Engineering, 70, 106345.

[32] Li, J., Cao, Y., Wang, Q., & Niu, B. (2019). Potential of Solar Heating for Ultra-Low-Energy Passive Buildings in Cold Regions. International Journal of Heat & Technology, 37(4).

[33] Zhang, D., Ding, Y., Wang, Y., & Fan, L. (2022). Towards ultra-low energy consumption buildings: Implementation path strategy based on practical effects in China. Energy for Sustainable Development, 70, 537-548.

[34] China Association of Building Energy Efficiency, Research Institute of Urban and Rural Construction and Development, & Chongqing University. (2024). China Building Energy Consumption and Carbon Emissions Research Report (2023). Architecture, (02), 46-59.

[35] The Central People's Government of the People's Republic of China. (2021, October 21). Opinions on Promoting Green Development in Urban and Rural Construction.

[36] Chen, B., & Liu, Y. (2013). Design and Evaluation of Passive Low-Energy Buildings. Construction Technology, 42(09), 99-101.

[37] GB/T 51366-2019. (2019). Standard for Calculation of Building Carbon Emissions (Standard). Beijing: China Architecture & Building Press.